

NUMERICAL SIMULATION OF FLUID-STRUCTURE INTERACTION BETWEEN FISHING WOBBLER AND WATER

**Miroslav Mijajlović¹, Sonja Vidojković^{2,3}, Dušan Ćirić¹,
Dragan Marinković¹**

¹University of Niš, Faculty of Mechanical Engineering, Serbia

²TU Delft, Faculty of Civil Engineering and Geosciences, Netherlands

³University of Belgrade, IHTM, Serbia

Abstract. *This paper deals with modeling, discretization, and numerical analysis of the two-way fluid-structure interaction between a fishing wobbler and a water stream. The structural domain is an assembly of several bodies that have multiple mutual structure-to-structure interactions. These interactions are mostly nonlinear contacts that significantly influence the time step used in simulations. As a result of these nonlinearities, the numerical solving of such a model requires significant computer resources and a long computational time. The paper also presents the creation and numerical simplifications of the model. However, the model remains very realistic. It is concluded that solving the structural domain in a model that retains the interaction between solid bodies is more computationally sensitive and more demanding than solving the fluid domain.*

Key Words: *Two Way Fluid-Structure Interaction, Fishing Wobbler, Structure Modeling, Contact Modeling, Fluid Modeling*

1. INTRODUCTION

The first artificial bait fishing probably occurred 2000 years ago in China or Mesopotamia, when fishers used a silk rope with a weighted bronze (shiny) hook as a fish bait [1]. These hooks were cast into the water and allowed to dive. Afterwards, the fishers would cyclically pull the rope, which would cause the hook to jiggle up and down. Such movement of the hook would create an illusion of an injured animal struggling to reach the water surface. Intrigued by the motion of an object resembling an easy meal, the predatory fish aggressively attacked the hook and became the prey.

Received January 28, 2020 / Accepted March 28, 2020

Corresponding author: Miroslav Mijajlović

University of Niš, Faculty of Mechanical Engineering, A. Medvedeva 14, 18000 Niš, Serbia

E-mail: miroslav.mijajlovic@masfak.ni.ac.rs

Artificial baits have evolved in many directions, and now there are hundreds of bait types. All of them behave differently in the water and target different species of fish. One group of artificial baits is well-known for its advantage represented by its complicated deflection in the water, as the preeminent action in luring the fish. The baits from this group are known as wobblers or crankbait [2].

During the initial diving, a wobbler wiggles in an irregular, oscillatory manner. When it reaches a quasi-equilibrium condition, it ceases to dive. Afterwards, the wobbler travels through the water predictably and oscillatorily. Such behavior is a result of a complex equilibrium of the forces that “surround” the wobbler [3].

This wobbler-water interaction is a typical example of fluid-structure interaction (FSI), where both the solid bodies and the fluids move. Govardhan et al. [4] modeled the swimming of a fish as FSI of the elastic body in the water. Their results show the disturbances of the water due to the Kármán vortex street effect. They used the dual-numeric equation solving methodology for full Newton–Raphson. Recently, Luo et al. [5] presented the effectiveness of a caudal peduncle-fin on a robotic fish model. They investigated it numerically using a fully coupled FSI, finite volume (FV) approach.

A comprehensive review of analytical and numerical FSI models applicable to the double-moving FSI is present in the works of Surana et al. [6], Chen and Zha [7] and Chakrabarti [8]. Several of the previously mentioned authors reported the limitations of commercial software as the main reason for the marginal application of numerical FSI. The software limitations were reflected in slow convergence, long calculation times, modeling contacts, mapping and meshing difficulties, and the number of executed iterations.

2. REAL WOBBLER AND ENVIRONMENT

The fishing wobbler looks like a predatory fish’s common prey – an insect, frog, small mammal, bird, squid, or fish. Therefore, the proper shape of the fishing wobbler is of importance for fishing success. Also, the fishing lure is surfaced and colored in such a manner as to get fish even more attracted. Usually, it has big eyes, almost always shiny and intense colors for major details, the bottom part of the wobbler is brighter than the top of the lure, etc. Wobblers are hollow with embedded noise-making parts inside the body (e.g. small steel balls), to attract the fish even more.

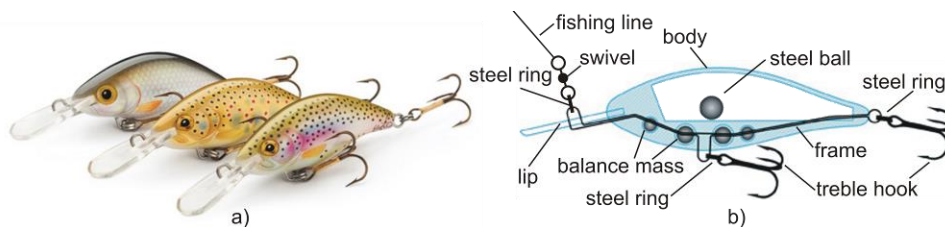


Fig. 1 Typical fishing wobbler: a) real model, b) detailed section view [9]

A typical small fish-like wobbler has a hollow body made of two symmetric, plastic or wooden pieces (left and right). The pieces are glued to each other in order to create a body. If necessary, the body is balanced with a certain amount of the contingency mass inserted at

prescribed locations. A steel wireframe, embedded into the body from the nose to the tail, reinforces the wobbler. The wobbler has a transparent diving lip at the nose of the lure. It is of a prescribed size, shape, position, and inclination concerning the wobbler's mass and shape. Usually, two treble hooks are attached to the frame at the tail and middle-belly of the wobbler. The small steel helical-shaped rings connect the hooks and the wireframe. The fishing line is tied to the swivel that has to prevent torsion of the fishing line. The swivel is, using a steel ring, mounted on the diving lip or wobbler's body [Fig. 1].

Afterwards, the prepared fishing line – wobbler fish system is used for fishing in the stagnant (standing) or flowing water (Fig. 2; Fig. 4, a and b). The goal is to enforce quasi-oscillatory movement of the wobbler in the water surroundings, in situations where the wobbler is not being pulled ($v_w=0$) and a water stream ($v_f \neq 0$) exists. The other two cases are when the wobbler is trolled ($v_w \neq 0$) in the standing water ($v_f=0$), or the wobbler is trolled/winded ($v_w \neq 0$) in the flowing water ($v_f \neq 0$).

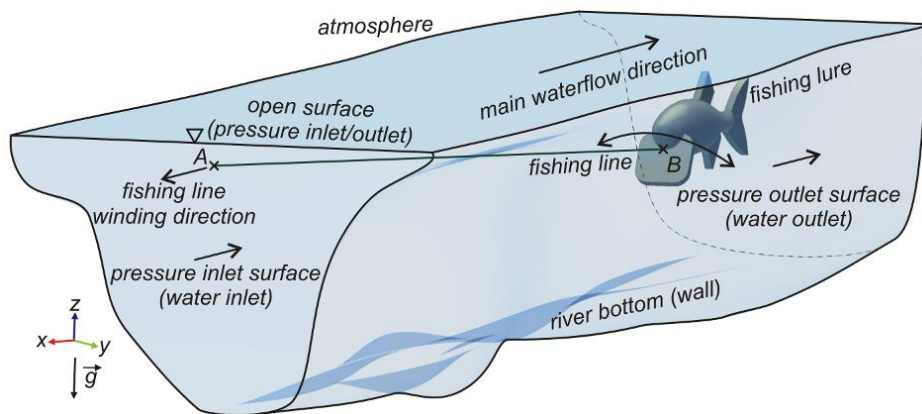


Fig. 2 The wobbler in the river

The interaction of the wobbler and the water generates forces that, combined with the gravity, hydrostatic pressure and mechanical force delivered by the fishing line, form an active force couple that moves the wobbler left-right and up-down in the water [3]. This exchange of the mutual influences of the water and the wobbler is FSI.

3. NUMERICAL MODEL

The first step in numerical modeling is to establish a computer-aided geometrical model (CAGM). For the shape of the wobbler, the small fish named “belica” (sunbleak or *Leucaspis delineates* in Latin) is adopted. The creating of CAGM combines the volumetric imaging methods (VIM) on *Leucaspis delineates* and assembling the other, standard, geometrical bodies (Fig. 3). As an assembly, they represent a solid (continuum) domain.

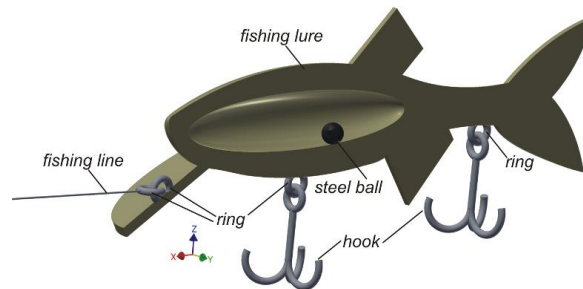


Fig. 3 The geometrical model of the wobbler and body interactions

The materials and properties of the bodies from the solid domain are given in Table 1.

Table 1 Parts, used materials, mechanical properties of materials

Part/Body...is made of...	Frame, hooks, rings, etc.	Fishing Line	Wobbler
Property / Name	Steel	Nylon	PA 6.6
Density (kg/m ³)	7850	1130	1150
Poisson's Ratio (-)	0.3	0.4	0.4
Young's Modulus (MPa)	200000	2000	3500
Bulk Modulus (GPa)	166.67	3.33	5.83
Shear Stress (GPa)	76.923	7.143	1.250
Yield Strength (MPa)	250	70	850
Ultimate Strength (MPa)	460	-	-

The fluid (continuum) domain (water) is modeled as a parallelepipedic environment surrounding the wobbler and accessories.

Both domains are modeled and discretized (meshed). The solid continuum is firstly simplified: the slim bodies (fishing line, treble hooks, rings, swivel) are modeled as 1D elements, while the massive bodies (wobbler and steel ball) are modeled as 3D elements. The usage of 1D elements in the structure modeling is not a novelty, but there are different opinions about its implementation in FSI. Gasche et al. [10] presented the FSI of a suction valve and a comparison of the 1D model to the 3D model regarding the computational time. They also observed a calculation time decrease of 15% in the model using 1D elements. Finally, they found the lack of stresses in line bodies (except axial stresses) [10].

3.1. Model discretization

The wobbler is modeled/discretized with 3D-high order Tet10 elements, while the fishing line and other accessories are modeled with beam elements. The mesh of the structural domain is stationary. The fishing line has a rounded cross-section of 0.25 mm in diameter, and it is 200 mm long. The water domain is dominantly discretized with linear 3D Tet4 elements while the water near the domain's boundary surfaces is discretized using thin prism-based elements (boundary layers, necessary to capture flow separation zones, velocity changes, etc.).

3.2. Structural model and constrains

All bodies from the solid domain have some mutual interactions: the steel ball occasionally hits the inner wall of the wobbler, the hooks interact with the rings, and sometimes they hit the outer wall of the wobbler; the fishing line is constrained at the free side while the other side is tied to the swivel, etc. These interactions are modeled as bonds, frictional contacts or joints with a certain degree of freedom restrained.

With all interactions involved, the numerical model of the wobbler and accessories is very complex and difficult for solving. It shows extreme nonlinear behavior that delivers convergence issues in simulation. Therefore, several simplifications are performed: the steel ball is neglected, and the 1D hook models are connected with the wobbler over one node (a 1D element's node is merged with a 3D element's node). The particular emphasis is set on modeling the interaction of the fishing line and the wobbler.

The real model joint between the fishing line and the fishing lure is over two metal rings where one ring is fixed to the fishing lure, and the fishing line ties the other ring. The ring-to-ring contact (Fig. 4, c) allows sliding that results in the weak restraining of the fishing lure: the fishing line does not enable the wobbler to flow away, but the wobbler can oscillate around its meta-stable position. Oscillation is possible around the main axis of the ring tied to the lure (axis 1), around the main axis of the ring tied to the line (axis 3), and only partially possible around the coplanar axis (axis 2). The relative translation of the rings is limited/minor due to the closed geometry of the rings – the fishing lure and the fishing line stay connected.

This relative positioning of the rings and the weak restraining of the fishing lure is one of the main reasons why the fishing wobbler can be guided through the water, leaving the ability to move like a wounded fish. Such a joining is quite difficult to be numerically modeled: one has to model a fixed joint between the fishing line and the ring, then a frictional contact/joint between (with specially constrained degrees of freedom) the two

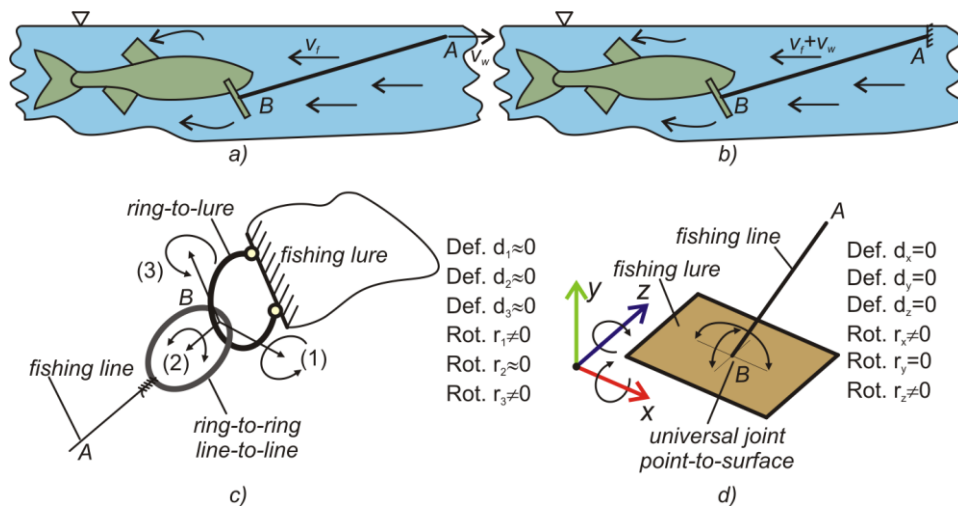


Fig. 4 The wobbler, water and accessories a) flowing water, winded wobbler, b) flowing water, constrained fishing line, c) fishing line to wobbler joint, d) universal joint

rings and a fixed joint between the second ring and the fishing lure. Such a configuration requires a very fine 3D mesh (or a combination of 1D and 3D), an extremely small time step (needed for convergence), and a powerful computer system. For those reasons, this configuration is simplified as the universal joint (Fig. 4, d) – the rings are neglected, the fishing line is modeled as a 1D structure, connected to the fishing lure as a point-to-surface universal joint. The local coordinate system is set to the contact point where the x-axis and the z-axis are tangent to the surface of the fishing lure, and the y-axis is normal. This universal joint restrains deformation/translation in all directions (x, y, z) and rotation in the y-direction, while rotation in the x-direction and the z-direction is free. The universal joint is a quite suitable representation of the real model: (x, y, z) directions are compliant to the (1, 2, 3) directions. The missing constraint is a partial rotation around the real model's (2) axis, which is fully constrained around the y-axis in the model. As a weakness of the model, it is neglected.

The only real constraining is achieved over the pulling point of the fishing line (A, Fig. 4, a and b). The point is pulling the fishing line and lure through the water at a certain speed, and the reactive force is creating equilibrium with all other forces that are loading the fishing lure. The real model concerns pulling the wobbler in one direction, while the water is flowing in the opposite direction. The model is simplified – the fishing line is not pulled (Fig. 4, b). Pulling point A in the numerical model is fixed (no rotation, no translation) but the flow rate of the water is increased for the value of the neglected pulling speed. Such behavior results in a smaller water continuum (faster calculation) and a more stable numerical model (the model with one or more fixation points becomes less sensitive to the rigid body motion).

3.3. Fluid model and constraints

The central part of the water domain follows the shape of the wobbler, and it ends at the boundary surfaces (bottom, riverside, water inlet and outlet, and air-interface). To effectively capture fluid-based phenomena near the solid body, the elements that represent fluid, near the wobbler, have to be small and of good quality.

For the fluid solver, the interface with the solid domain is a rough, movable, coupled wall. The bottom and riverside are static, rough walls. All the remaining surfaces are pressure and velocity based boundaries, without surface roughness (no-slip walls) (Fig. 2). The water enters the water domain through the inlet surface, and leaves it from the outlet surface, while the free surface is a constant pressure-based wall. This representation of the free surface is an imprecise simplification of the open channel flow (density 998 kg/m³, total pressure 1.01325 MPa, at 0 m altitude and temperature of 20°C). The maximal depth/height of the water domain is 250 mm, and the nominal water-flow through the domain is 0.4 m/s.

The surface roughness at the walls is modeled using the equivalent Sand-Grain Roughness [11, 12]. To accurately capture the fluid separation near the boundaries, the mesh generator creates prism elements as layers near the boundary walls. The size and the number of layers are selected to provide the y^+ wall distance for the predicted high Reynolds y^+ treatment [13, 14].

The fluid flow numerical model is a transient, pressure-based model, without gravity. The contact stress is defined as constant surface tension stress. The turbulence in the fluid is modeled using the realizable k- ϵ model (2 transport equations). The model uses scalable

wall functions (it benefits from the prism elements) for the near-wall treatment and estimation of fluid velocities in the border layers.

The solution is obtained using a pressure-velocity coupling scheme, with a second-order upwind discretization scheme for solving Reynolds Average Navier-Stokes (RANS) equations. The coupled “PRESTO!” scheme defines the pressure estimation in the fluid domain. The compressed volume fraction estimation scheme with the transient first-order implicit formulation is active, as well.

4. FSI MODELING

The solid domain and the fluid domain have a strong, mutual, two-way interaction: the fishing lure (solid domain) influences the water (fluid domain) by pure mechanical deformation of the fluid continuum. The fluid continuum – water changes some of its parameters (e.g. pressure), which results in the appearance of the forces that act on the fishing lure. The forces tend to reach equilibrium, and as a result of this tendency, the fishing lure moves. This equilibrium is the basis of the two-way fluid-structure interaction.

Numerically, FSI is a set of calculations within the discretized domains in discretized time intervals (steps). Initially, a set of equations from one of the domains is calculated (either structural or fluid) for the initial time ($t=0$ s), the results are transferred to the other set of equations (the ones of the domain that is not calculated), and then the equations are solved (Fig. 5). The FSI module checks the convergence, mapping, and precision of the data transfer. Afterwards, time is increased for the value of the time step ($t+\Delta t$, $\Delta t=0.001$ s), and the calculation procedure is repeated. This procedure is repeated until the end of the prescribed time ($t_{max}=10$ s). Selecting the proper time step is a complicated task. One approach is to choose it in a manner of preserving the quality of the generated mesh [15]. In the presented case, the time step is selected intuitively.

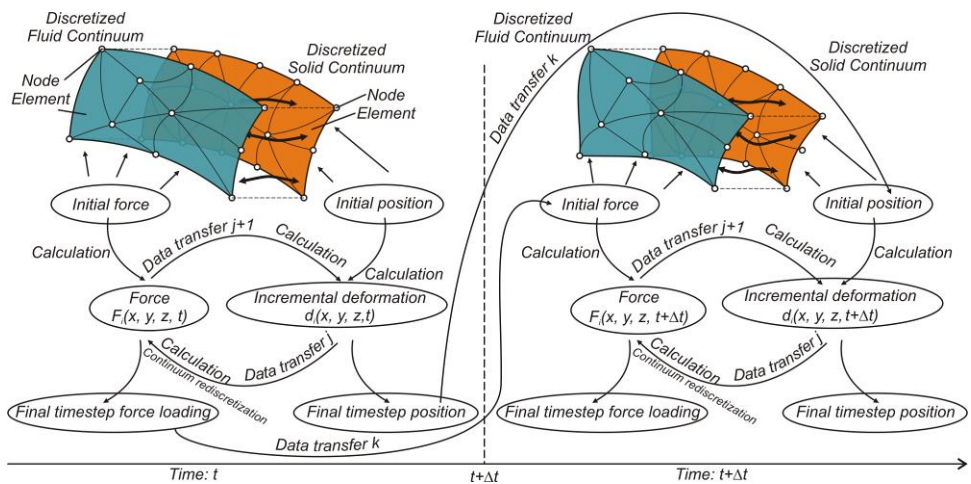


Fig. 5 FSI schematic

5. RESULTS AND DISCUSSION

The movement of the wobbler in the water appears to be oscillatory and complex. The wobbler shows a tendency to dive and slightly emerge towards the water surface, while the left-right twisting pushes the wobbler downward. For the understanding of the wobbler's wiggling movement, eight characteristic points on the wobbler are defined, and each of them is defined with the hodograph (Fig. 6).

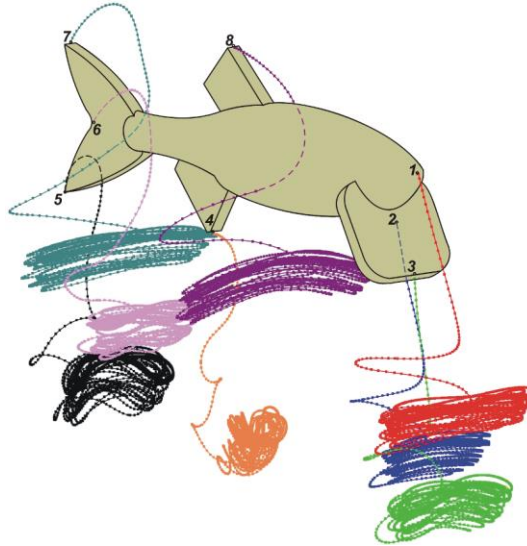


Fig. 6 The hodograph of the characteristic points (ISO view)

At the initial time, the wobbler starts to dive until it “mounts” the equilibrium location. It does not show any oscillatory movement before that. Afterwards, it starts to oscillate regularly to the $\pm z$ -direction (Fig x), deflecting up to 30 mm (points 7 and 8 in Fig. 6).

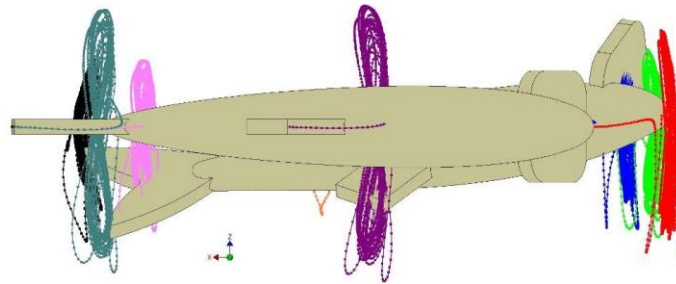


Fig. 7 The hodograph of the characteristic points (XZ plane view)

The majority of the points (points 4 to 8, Fig. 6) create almost twisted hodographs (shaped like the number eight), while the rest of the points have different hodograph patterns.

The wobbler's body suffers very low stresses (Fig. 8). Such behavior is expected since the wobbler is not constrained ordinarily. When the forces emerge on the wobbler's body, it bends/deflects slightly and evades the loading. Regardless of this fact, the simulation shows that the extreme values of stresses appear at the roots of the wobbler fins and the universal joint.

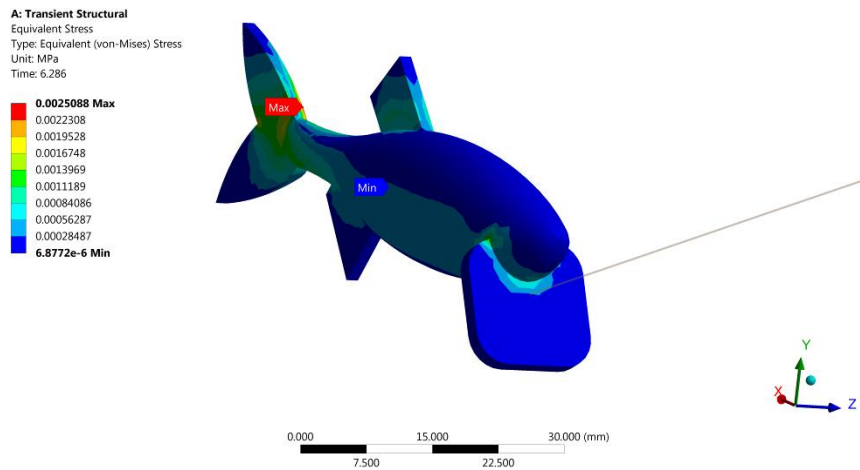


Fig. 8 The Von Mises stress in the wobbler

The water flow shows a typical eddy behavior around the swimming wobbler (Figs. 9 and 10). It reaches the maximal flow of 0.539 m/s in a vortex near the wobbler's left side, at the time moment of 4.8 s.

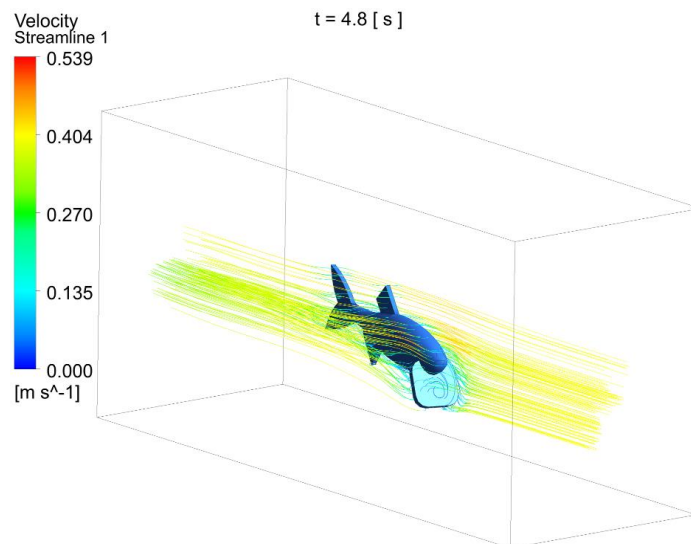


Fig. 9 The velocity streamline

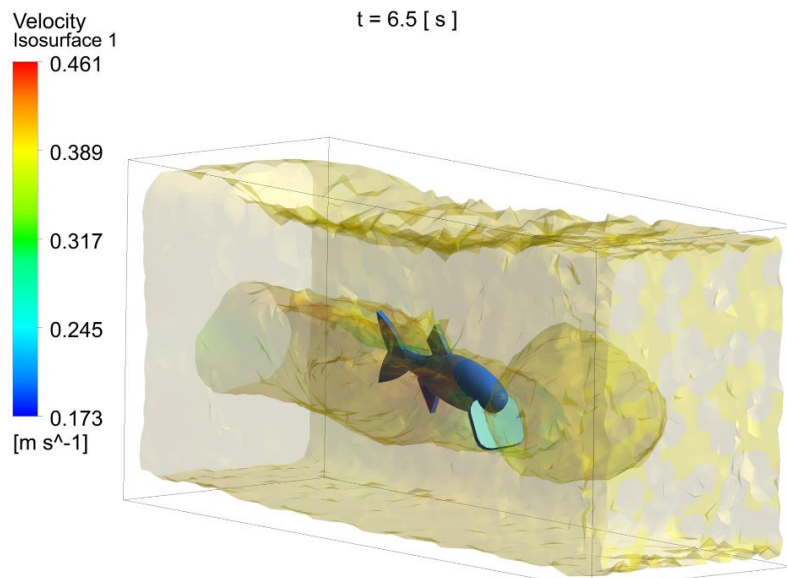


Fig. 10 The velocity isosurface of 0.4 m/s

The velocity isosurface (set on the nominal value of 0.4 m/s, Fig. 10) shows that the diving lip produces a significant water-flow disturbance effect. In this manner, it is the major component of the wobbler that defines the wobbler's deflection. It seems that it should be smaller and less edgy than it is in this configuration (Fig. 10).

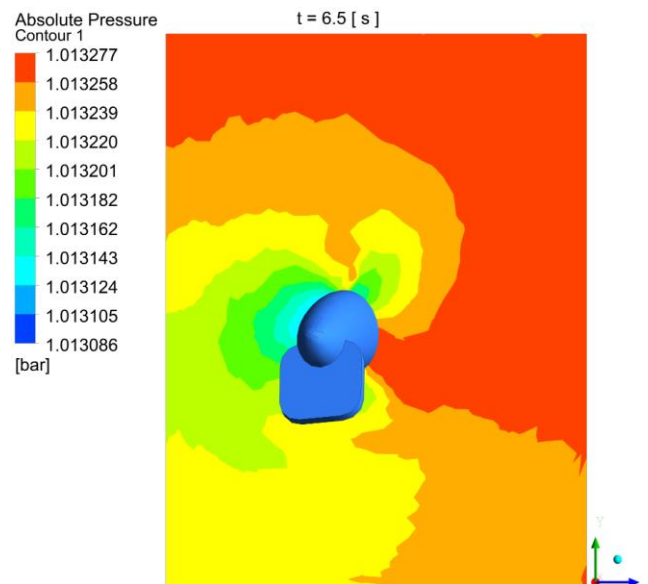


Fig. 11 The absolute pressure contour plot in plane $x=20$ mm

The contour plot of the water's absolute pressure shows a vortex effect in the lateral direction of the wobbler (Fig. 11). There is no excessive increase or decrease of the pressure around the wobbler's body (max 0.5%). However, this slight change of pressure causes the significant deflection of the wobbler.

6. CONCLUSIONS

The preparations of the numerical model, initial simulations, and final results showed several different contradictory facts about the modeling and simulation of such an FSI case.

Initially, the numerical modeling of the structure and body interactions in the structure appeared to be a challenging and significant convergence issue. Due to them, the time step had to be drastically decreased. It might be useful to neglect many of them or somehow to "linearize" them.

Modeling and preserving the fish fins in simulation influences the pattern of the wobbler's deflection in the water. Visually, the wobbler has more fish-like topography, but it is questionable how much the preserved fins affect the fishing success of the wobbler. Furthermore, as thin bodies, they can easily get broken in real fishing.

Neglecting gravity and simulating the air pressure as constant (to avoid calculating the time-demanding open-channel flow and volume of the fluid approach), affects the precision of the results. However, if only a global picture of the interaction is essential, they can be neglected. The boundary layer modeling (for capturing the flow-separation effect near the walls) should not be neglected. Moreover, it has to be modeled very carefully.

REFERENCES

1. New World Encyclopedia, 2019, *Fishing lure*, https://www.newworldencyclopedia.org/entry/Fishing_lure (accessed 09 October 2019).
2. Fishingnoob, 2019, *Types of Fishing Lures*, <http://fishingnoob.com/68/types-of-fishing-lures/> (accessed 09 October 2019).
3. Mijajlović, M., Ćirić, D., 2018, *Two way coupled fluid-structure interaction analysis of the grasshopper fishing lure's movement in the water stream*, Proc. The 4th International Conference Mechanical Engineering in XXI Century - MASING 2018, Niš, Serbia.
4. Govardhan, D., Ramulu, P.J., Prasad, P.V.S.R., Anbusagar, N.R.R., 2018. *Hydrodynamics of a fish using fluid structure interaction*, Materials Today: Proceedings, 5, 13, Part 3, pp. 27205-27212.
5. Luo, Y., Xiao, Q., Shi, G., Yuan, Z., Wen, L., 2019. *A fluid-structure interaction study on a passively deformed fish fin*, Proc. ASME 2019, 38th International Conference on Ocean, Offshore and Arctic Engineering, OMAE 2019, Glasgow, United Kingdom, 9/06/19 - 14/06/19.
6. Surana, K.S., Blackwell, B., Powell, M., Reddy, J.N., 2014. *Mathematical models for fluid-solid interaction and their numerical solutions*, Journal of Fluids and Structures, 50, pp. 184-216.
7. Chen, X.Y., Zha, G.C., 2005, *Fully coupled fluid-structural interactions using an efficient high resolution upwind scheme*, Journal of Fluids and Structures, 20, 8, pp. 1105-1125.
8. Chakrabarti, S.K., 2005, *Numerical Models in Fluid-Structure Interaction*, WIT Press, Offshore Structure Analysis Inc., USA.
9. Ujka Vobleri, 2019, *BD4*, <http://ujkavobleri.com/ujka/model-bd4.html#video>, (accessed 09 October 2019).
10. Gasche, J.L., Dias, A.D.S.L., Bueno, D.D., Lacerda, J.F., 2016, *Numerical simulation of a suction valve: comparison between a 3D complete model and a 1D model*, Proc. 23rd International Compressor Engineering Conference at Purdue, pp. 2-8.
11. Tauviqirrahman, M., Ichsan, B.C., Jamari, M., 2019, *Influence of roughness on the behavior of three-dimensional journal bearing based on fluid-structure interaction approach*, Jour. Mech Sci Technol, 33, pp. 4783.

12. Adams, T., Grant, C., Watson, H., 2012, *A simple algorithm to relate measured surface roughness to equivalent sand-grain roughness*, International Journal of Mechanical Engineering and Mechatronics, 1(1), pp. 66-71.
13. Terziev, M., Tezdogan, T., Oguz, E., Gourlay, T., Demirel, Y.K., Incecik, A., 2018, *Numerical investigation of the behaviour and performance of ships advancing through restricted shallow waters*, Journal of Fluids and Structures, 76, pp. 185-215.
14. Ansys Support, 14.5 Release, 2012. *Lecture 7: Turbulence. Introduction to ANSYS Fluent*, Ansys.
15. Konyukhov, A., Izi, R., 2015, *Introduction to Computational Contact Mechanics: A Geometrical Approach*, Wiley Series in Computational Mechanics, John Wiley & Sons, Chichester, UK.